PHYSICAL REVIEW B **88**, 081107(R) (2013)

Local moments and suppression of antiferromagnetism in correlated $Zr_4Fe_4Si_7$

J. W. Simonson,[1,*] M. E. Pezzoli,[1,2] V. O. Garlea,[3] G. J. Smith,[1] J. E. Grose,[1] J. C. Misuraca,[1] G. Kotliar,[2] and M. C. Aronson[1,4]

[1]*Department of Physics and Astronomy, Stony Brook University, Stony Brook, New York 11794, USA*

[2]*Department of Physics and Astronomy, Rutgers University, Piscataway, New Jersey 08854, USA*

[3]*Quantum Condensed Matter Division, Oak Ridge National Laboratory, Oak Ridge, Tennessee 37831, USA*

[4]*Condensed Matter Physics and Materials Science Department, Brookhaven National Laboratory, Upton, New York 11973, USA*

(Received 5 July 2013; revised manuscript received 16 August 2013; published 29 August 2013)

We report magnetic, transport, and neutron diffraction measurements as well as a doping study of the V-phase compound $Zr_4Fe_4Si_7$. This compound exhibits collinear antiferromagnetic order below $T_N = 98 \pm 1$ K with a staggered moment of $0.57(3)\mu_B$/Fe as $T \to 0$. The magnetic order can be quenched with Co substitution to the Fe site, but even then a $1.5\mu_B$/Fe paramagnetic moment remains. The resistivity and heat capacity of $Zr_4Fe_4Si_7$ are Fermi-liquid-like below 16 and 7 K, respectively, and reveal correlations on the scale of those observed in superconducting Fe pnictides and chalcogenides. Electronic structure calculations overestimate the ordered moment, suggesting the importance of dynamical effects. The existence of magnetic order, electronic correlations, and spin fluctuations make $Zr_4Fe_4Si_7$ distinct from the majority of Fe-Si compounds, fostering comparison instead with the parent compounds of Fe-based superconductors.

DOI: 10.1103/PhysRevB.88.081107 PACS number(s): 75.25.−j, 75.50.Ee, 75.30.−m, 72.15.Eb

It is believed that the pairing mechanism in the Fe pnictide and chalcogenide superconductors stems from spin fluctuations associated with proximity to a magnetic phase boundary.[1–4] The Fe tetrelides, composed of anions of group 14, often take the same crystal structures as these compounds. They have not been found to manifest high temperature superconductivity, however, and in most cases lack even Fe-based magnetic order. While superconducting Fe tetrelides have been reported—notably $Lu_2Fe_3Si_5$ ($T_c = 6.1$ K) and related compounds[5] as well as $YFe_{2-\delta}Si_2$ ($T_c = 3$ K), which is isostructural with $BaFe_2As_2$ (Ref. 6)—correlations in these materials are often minimal, and their superconducting states do not appear to be associated with Fe magnetism.[7–10]

$Zr_4Fe_4Si_7$ is an Fe tetrelide that forms in the tetragonal, ringlike V-phase structure.[11] While this structure type has been known for decades,[12] most studies of V-phase compounds to date have focused on crystallography,[13] and it is not yet known if these materials exhibit magnetic order or superconductivity. Nonetheless, resonant photoemission measurements on $Ti_4M_4Si_7$ (M = Co, Ni)[14] found the top of the valence band to be dominated by M-3d states, suggesting proximity to magnetism. Moreover, core level spectroscopy suggested that both compounds are metallic and, most interestingly, that replacing Ni with Co or Fe would lead to enhanced electronic correlations.[14]

We synthesized single crystals of $Zr_4Fe_4Si_7$ and via magnetic and neutron measurements found this compound to be a rare example of an Fe tetrelide with magnetic order. Transport measurements and electronic structure calculations revealed enhanced correlations similar in magnitude to those present in the parent compounds of Fe superconductors. Perhaps most interestingly, the onset of magnetic order in $Zr_4Fe_4Si_7$ can be suppressed to lower temperatures with Co doping, even as the Curie-Weiss moment remains large, revealing that the collapse of magnetic order in this compound is not due to the abatement of the moments. This combination of magnetic order with a robust paramagnetic moment makes $Zr_4Fe_4Si_7$ distinct from the typically uncorrelated Fe tetrelides but is more characteristic of the Fe pnictide and chalcogenide superconductors.[15]

We grew lustrous, acicular crystals of $Zr_4Fe_4Si_7$ as large as $0.2 \times 0.2 \times 12$ mm^3 from a solution with an atomic ratio of 4:4:7:735 (Zr:Fe:Si:Ga). The crystals were cleaned with HCl, and the structure was confirmed with x rays. Compositions were verified by energy dispersive x-ray spectrometry with a JEOL 7600F analytical SEM. The dc susceptibility of a batch of crystals mutually oriented along their c axes and wrapped in Au foil was measured from 1.8 to 400 K in a Quantum Design Magnetic Properties Measurement System (MPMS). Resistivity was measured with a 1 μA ac current along the c axis in a Quantum Design Physical Properties Measurement System (PPMS) from 0.42 to 300 K. Heat capacity was measured from 1.8 to 300 K in a PPMS. Neutron diffraction from a polycrystalline sample prepared via solid state reaction was done at beamline HB-2A of the High Flux Isotope Reactor between 4 and 140 K using wavelengths $\lambda = 1.538$ and 2.41 Å. The magnetic structure was determined via representational analysis with FULLPROF and SARAh.[16,17] Electronic structure calculations were carried out using the all electron linearized augmented plane wave (LAPW) method as implemented in the WIEN2K code.[18] We used the Perdew-Burke-Ernzerhof parametrization of the exchange-correlation potential in the generalized gradient approximation (GGA).[19] The number of k points in the irreducible Brillouin zone was 110 for a total of 1600 k points, and $R_{mt} \star K_{\max} = 9.0$.

Figure 1 shows the magnetic and physical properties of $Zr_4Fe_4Si_7$, revealing order at 98 K. In Fig. 1(a) we plot the dc magnetic susceptibility $\chi = M/H$ with a field $H = 1$ T oriented both parallel and perpendicular to the c axis. In both cases, a maximum corresponding to the onset of order occurs at 98 ± 1 K. Anisotropy in χ is modest, being $\lesssim$10% for all T investigated. As we show in Fig. 1(b), χ falls off above the ordering temperature, obeying the Curie-Weiss law for $T \gtrsim$ 200 K and yielding a fluctuating moment $p = 2.0(1)\mu_B$/Fe. This moment is larger than expected for an $S = 1/2$ low-spin Fe state but is too small for intermediate spin configurations

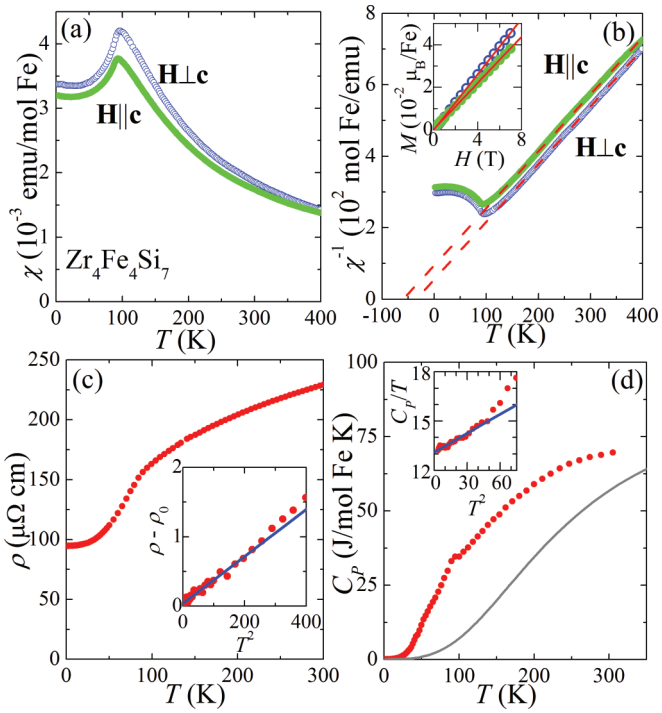

FIG. 1. (Color online) (a) The temperature dependence of the susceptibility χ of $Zr_4Fe_4Si_7$ with a 1 T dc field $\mathbf{H} \perp \mathbf{c}$ (open blue circles) and $\mathbf{H} \parallel \mathbf{c}$ (filled green circles). (b) The temperature dependence of $1/\chi$ with $\mathbf{H} \perp \mathbf{c}$ (open blue circles) and $\mathbf{H} \parallel \mathbf{c}$ (filled green circles). The red dashed lines are fits to the Curie-Weiss law. Inset: At $T = 1.8$ K, magnetization $M(H)$ is linear in both orientations. Solid red lines are best linear fits. (c) The temperature dependence of the resistivity ρ. Inset: ρ-ρ_0 is linear in T^2. The solid blue line is the best linear fit. (d) The heat capacity C_P as a function of T (filled red circles) and the Debye heat capacity C_{lattice} with Debye temperature $\theta = 900 \pm 25$ K (gray line). Inset: C_P/T vs T^2 for $T < 9$ K. The solid blue line is the best linear fit.

with $S = 1$ or larger, suggesting that Fe-3d hybridization reduces p from the free ion value. The Weiss temperature Θ_W varies from -34 to -60 K depending on orientation, with the negative sign indicative that the dominant exchange is antiferromagnetic. The inset of Fig. 1(b) plots magnetization M versus H at $T = 1.8$ K, which displays no saturation in $H \leqslant 7$ T. This linearity is consistent with the absence of ferromagnetism. Overall, these data indicate that $Zr_4Fe_4Si_7$ is an antiferromagnet with $T_N = 98 \pm 1$ K.

The resistivity ρ and heat capacity C_P confirm the onset of order at T_N. In Fig. 1(c), we show that ρ increases with T, revealing $Zr_4Fe_4Si_7$ to be a metal. The slope of $\rho(T)$ increases abruptly as the sample is cooled through T_N. The inset shows that $\rho - \rho_0 \propto T^2$ when $T \leqslant 16$ K with proportionality constant $A = 3.4 \times 10^{-3}$ $\mu\Omega$ cm/K^2, where ρ_0 is the resistivity at $T = 0.42$ K, indicating Fermi-liquid-like behavior. There is no indication of superconductivity above 0.42 K. A feature at T_N is also visible in the C_P data presented in Fig. 1(d), indicating that the transition is likely to be bulk. At 300 K, C_P falls short of the 177 J/mol Fe K Dulong-Petit limit, suggesting that the Debye temperature θ is substantially higher. The inset shows a linear relationship between C_P/T and T^2 for $T \leqslant 7$ K, yielding $\theta = 900 \pm 25$ K.

The calculated phononic contribution C_{lattice} obtained from θ significantly underestimates the measured C_P, and we presume the excess $C_\Delta = C_P - C_{\text{lattice}}$ is in part due to magnetic interactions. The linear relationship between C_P/T and T^2 also allows for isolation of the electronic contribution $\gamma = 13$ mJ/mol Fe K^2, reflecting moderate mass enhancement over the $\gamma = 6$–9 mJ/mol Fe K^2 reported for the $R_2Fe_3Si_5$ superconductors[10] and more substantial enhancement over the $\gamma = 1$–3 mJ/mol Fe K^2 reported for binary Fe-Si compounds.[20] In comparison, quasiparticle masses in the Fe pnictides are enhanced by a factor of 2 to 3 above the free electron value.[4] Thus, while measurements of ρ and C_P confirm the magnetic transition, their behavior as $T \to 0$ reveals that $Zr_4Fe_4Si_7$ fosters reasonably strong electronic correlations.

The magnetic structure determined by neutron diffraction is presented in Fig. 2. In Fig. 2(a) we show a refinement at $T = 4$ K and $\lambda = 1.538$ Å. Patterns obtained below T_N include a single magnetic peak at $Q = 1.08$ Å^{-1}, which is indexed by the propagation vector $\mathbf{k} = (0,0,1)$, indicating that the body-centered symmetry of the nuclear structure is not present in the magnetic structure. The nuclear space group $I4/mmm$ contains 16 operations, all of which leave $\mathbf{k}$ invariant. The magnetic representation of the Fe site can be decomposed to a series of irreducible representations (IRs)[21] of the group of these 16 operations. This decomposition yields ten IRs, which were compared to the data. Only one IR, Γ_7 by Kovalev's tables,[22] proved suitable for modeling the pattern. The model in Fig. 2(a) was generated from refinement of the

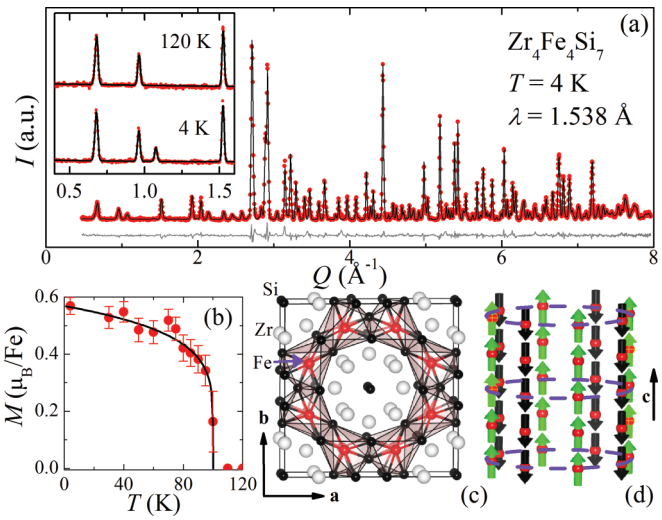

FIG. 2. (Color online) (a) Rietveld refinement (black line) of the diffraction pattern (red circles) of $Zr_4Fe_4Si_7$ collected with 1.538 Å neutrons at 4 K. The difference curve is shown below in gray. The inset shows the single magnetic peak below T_N. (b) Temperature dependence of the ordered moment M. The black line is a power law fit (see text) assuming $T_N = 100$ K and yielding critical exponent $\beta = 0.17(3)$. (c) The unit cell viewed down the c axis. Linear chains of Fe (red) and tubes of Zr (white) are arranged in rings and coordinated by Si (black), as indicated. (d) The magnetic structure with Zr and Si atoms omitted. Fe atoms (red) lie in chains along $\mathbf{c}$, and their moments are parallel (green) and antiparallel (black) to the c axis. The purple dashed rings establish perspective.

nuclear structure and the magnitudes of the two basis vectors associated with Γ_7.

Figure 2(b) shows the refined static moment M at several temperatures. Magnetic intensity appears below T_N, and M reaches a value of $0.57(3)\mu_B$/Fe as $T \to 0$. We fit these data with a power law $M \propto t^\beta$, where reduced temperature $t = (T - T_N)/T_N$. The critical exponent $\beta = 0.17(3)$ is substantially smaller than those of three-dimensional mean field ($\beta = 0.5$) and Heisenberg and Ising universality classes ($\beta \simeq 0.33$), giving an overly sharp curvature and suggesting that the transition may have either some degree of first order character or reduced dimensionality.[23] Figure 2(c) depicts the crystal structure and Fig. 2(d) the magnetic structure. Chains of moments coalign along **c**, and neighboring chains are antialigned, resulting in an antiferromagnetic configuration. The moment along **c** stems from one of the two basis vectors associated with Γ_7. The second vector would cant the moments. While permitted by symmetry, a nonzero magnitude for this vector does not improve the refinement, and we observe no indication of peaks that would support this possibility. Even if we cannot rule out that these peaks are present, the level of the background constrains the canting angle to $\lesssim 10^\circ$. In sum, $Zr_4Fe_4Si_7$ exhibits a simple magnetic structure and both a modest T_N and $T \to 0$ moment, similar to those of the Fe pnictides.[24] Analogously, we expect that superconductivity would require suppression of this antiferromagnetic state.

We show in Fig. 3 that magnetic order in $Zr_4Fe_4Si_7$ is suppressed by Co doping. Figure 3(a) plots χ of $Zr_4Fe_4Si_7$, $Zr_4Co_4Si_7$, and several intermediate compositions

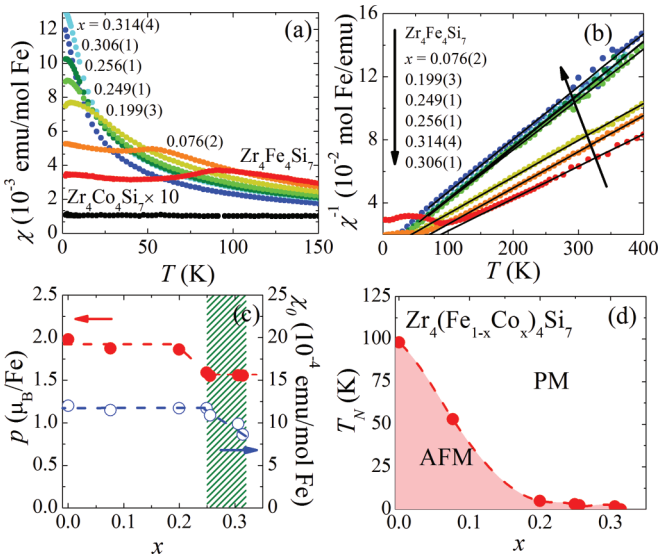

FIG. 3. (Color online) (a) The temperature dependence of the susceptibility χ of $Zr_4(Fe_{1-x}Co_x)_4Si_7$, where $x = 0$ (red), $x = 0.076(2)$ (orange), $x = 0.199(3)$ (yellow), $x = 0.249(1)$ (light green), $x = 0.256(1)$ (dark green), $x = 0.306(1)$ (light blue), $x = 0.314(4)$ (dark blue), and $x = 1$, i.e., $Zr_4Co_4Si_7$ (black). (b) The reciprocal susceptibility, colors as in (a), as indicated. Solid black lines are fits to the Curie-Weiss law. (c) The Curie-Weiss moment p (left, filled red circles) and the temperature independent susceptibility χ_0 (right, open blue circles) as a function of composition x. The shaded green area highlights the region leading up to the $T = 0$ phase transition. (d) The magnetic phase diagram of $Zr_4(Fe_{1-x}Co_x)_4Si_7$.

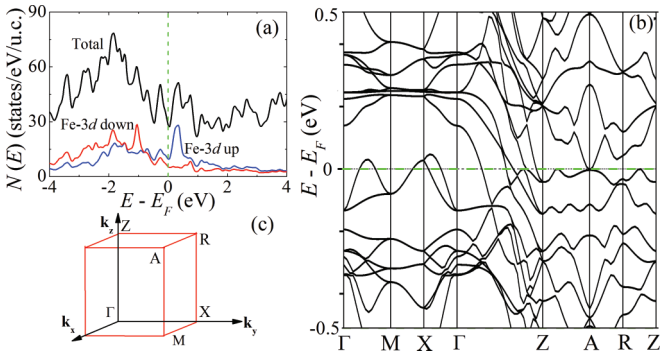

FIG. 4. (Color online) (a) The total (black), Fe 3d-up (blue), and Fe 3d-down (red) densities of states $N(E)$ of $Zr_4Fe_4Si_7$, as indicated. (b) The electronic structure plotted along several high symmetry directions of (c) the magnetic space group $P4/mnc$ (Ref. 29).

$Zr_4(Fe_{1-x}Co_x)_4Si_7$ ($0.076 \leqslant x \leqslant 0.314$). For $Zr_4Fe_4Si_7$, χ includes a cusp at T_N and Curie-Weiss behavior at higher T. For $Zr_4Co_4Si_7$, χ is independent of T and at least 20 times smaller, suggesting that the Co atoms have no moment. As x increases, the cusp at T_N shifts to lower T, but no superconductivity is observed above 1.8 K for any x. Plots of $1/\chi$ in Fig. 3(b) reveal agreement with the Curie-Weiss law for all $x < 1$. The slope of $1/\chi$ exhibits a steplike decrease with x, as depicted in Fig. 3(c). For $0 \leqslant x \leqslant 0.199$, the effective moment p is nearly unchanged from $2.0(1)\mu_B$/Fe, even as T_N is suppressed from 98 to 5 K [Fig. 3(d)]. For $0.249 \leqslant x \leqslant 0.314$, however, p takes a new value near $1.5\mu_B$/Fe, and the reduction of T_N with x slows. The temperature independent susceptibility χ_0 remains constant with x until p drops, whereupon it likewise begins to decrease. Here χ_0 is plotted per Fe atom, suggesting that the contribution of Co to the density of states at the Fermi level $N(E_F)$ is minimal. Only by $x \simeq 0.3$ is $N(E_F)$ per Fe apparently reduced by doping. The magnetic phase diagram appears in Fig. 3(d).

Figure 4 presents the GGA electronic structure of $Zr_4Fe_4Si_7$. We show in Fig. 4(a) the total and spin polarized Fe-3d densities of states $N(E)$. The majority of $N(E)$ near E_F is of Fe-3d character, but we observe significant Zr-4d contribution. Substantial Fe-3d spin polarization is present, yielding a calculated moment of $1.08\mu_B$/Fe—an overestimate of the neutron moment by a factor of ~ 2. Even a calculation performed within the local spin density approximation, which typically underestimates the moment,[25] finds $0.87\mu_B$/Fe. These significant overestimates suggest that the experimental moment is reduced by correlations beyond the static mean field exchange. Overestimate of the static moment by density functional theory has been recently examined for Fe pnictides and chalcogenides and has been explained as the result of quantum fluctuations, which may originate from proximity to a quantum critical point.[25,26] Results in these systems also show large sensitivity to the method of approximating the exchange-correlation functional,[27] just as we find here. It is likely that $Zr_4Fe_4Si_7$ may also fall into the class of Hund's metals, in which correlations stem from Hund's coupling rather than solely from the Hubbard U. Hund's metals are characterized by strong charge fluctuations, and their moments are likewise overestimated by static mean field theories.[26,28] In Fig. 4(b) we plot the electronic structure of $Zr_4Fe_4Si_7$ along

several high symmetry directions, as defined in Fig. 4(c).[29] The bands are nearly dispersionless along Γ-*M*-*X*-Γ, i.e., within the *ab* plane, suggesting that the charge carriers are heavy. Meanwhile five bands are active along the Γ-*Z* ($\mathbf{k}_z$) direction, and their bandwidth is large, ∼0.4 eV. As we saw for Γ-*M*-*X*-Γ, the dispersion across the top face of the Brillouin zone is again relatively small. This strong anisotropy is interesting given that χ is relatively isotropic, suggesting that the moments are derived from states far from E_F.

The transport and magnetic data also show evidence of strong correlations. The Kadowaki-Woods ratio $R_{KW} = A/\gamma^2$,[30] which compares the temperature dependencies of the resistivity and heat capacity in a Fermi liquid, comes to 20 $\mu\Omega\,\mathrm{cm\,mol^2\,K^2\,J^{-2}}$, twice as large as the typical number for heavy fermion compounds.[30] This large R_{KW} is symptomatic of strong correlations,[31] and indeed $Zr_4Fe_4Si_7$ has an R_{KW} between those of the unconventional superconductors $La_{1.7}Sr_{0.3}CuO_4$ and Sr_2RuO_4.[32] In comparison, the superconductor KFe_2As_2 has a slightly smaller $R_{KW} \approx 14\ \mu\Omega\,\mathrm{cm\,mol^2\,K^2\,J^{-2}}$,[33] while values for optimally doped Fe pnictides are higher still.[34,35] The Sommerfeld-Wilson ratio $R_{SW} = K\chi_0/\gamma$, for which $R_{SW} = 1$ corresponds to a free electron gas, gives an enhanced value of $R_{SW} \simeq 7$ for $Zr_4Fe_4Si_7$, nearly the same as for Pd.[36] Here $K = 4\pi^2 k_B^2/3(g\mu_B)^2$, where the Landé g factor $g = 2$, $\chi_0 = 1.2 \times 10^{-3}$ emu/mol Fe [Fig. 3(c)], and $\gamma = 13$ mJ/mol Fe K^2 [Fig. 1(d)]. This ratio indicates that χ_0 is more strongly enhanced by the correlations than is γ, suggesting that ferromagnetic spin fluctuations are present. We posit that these fluctuations may be related to the coaligned moments of nearest neighbor Fe atoms along the *c* axis.

Putting together the experimental results with the electronic structure, we begin to develop a cohesive picture of $Zr_4Fe_4Si_7$. In the pnictides and chalcogenides, superconductivity arises as magnetic order is extinguished. Our observations of $Zr_4Fe_4Si_7$ reveal moderately heavy quasiparticles, spin fluctuations, and the suppression of order with doping, suggesting that similar physics may be present in this compound, yet doping with Co does not yield a superconducting state. We put forth three reasons why this may be the case. First, p remains nearly invariant at $1.5\mu_B$/Fe even as $T_N \to 0$ K. The local fields associated with these well formed moments could potentially provide a pair-breaking mechanism. It is interesting that the moment in the undoped compound is $2.0(1)\mu_B$/Fe, almost exactly the sum of the $0.57(3)\mu_B$/Fe ordered moment and the moment that remains after T_N is suppressed with doping, as if the fluctuating component is decoupled from the electronic structure and is thereby unaffected by charge doping. X-ray emission spectroscopy measurements have revealed, however, that local magnetic moments on the order of $1–3\mu_B$/Fe persist deep into the paramagnetic state of the Fe pnictides,[15] suggesting that their presence need not be the death knell for superconductivity. Second, the electronic structure of $Zr_4Fe_4Si_7$ is both more complicated and more anisotropic than those of the Fe pnictides, and the Fermi surface, unlike those of the pnictides, has no clear nesting vector. Third, and perhaps most important, a large R_{SW} reveals that the very spin fluctuations thought to generate superconductivity in the pnictides are in this case ferromagnetic, serving instead to discourage the formation of Cooper pairs. It may be the V-phase structure, and specifically the linear chains of Fe atoms, that is ultimately responsible for all three of these phenomena. It is possible that the atomic site disorder introduced by doping Co atoms into these one-dimensional chains serves to preserve both the fluctuating local moments and their tendency towards coalignment even in the absence of order.

While $Zr_4Fe_4Si_7$ hosts correlations and tunable magnetic order, the moments are perhaps too local and the spin fluctuations too ferromagnetic to kindle superconductivity. On the other hand, many of the Fe tetrelides, apparently including those isostructural with high T_c superconductors, are too weakly correlated to foster Fe-based magnetism.[10,20] $Zr_4Fe_4Si_7$ provides a rare example of an Fe tetrelide in which there are large Fe moments as well as antiferromagnetic order, revealing that the tetrelides, like the Fe pnictides and chalcogenides, inhabit a spectrum that encompasses local moment magnets to itinerant metals, somewhere in the middle of which presumably lies superconductivity.

Work at Stony Brook University and Rutgers University was carried out under the auspices of a Department of Defense National Security Science and Engineering Faculty Fellowship via the Air Force Office of Scientific Research. Research at Oak Ridge National Laboratory's High Flux Isotope Reactor was sponsored by the Scientific User Facilities Division, Office of Basic Energy Sciences, US Department of Energy. Research at the Center for Functional Nanomaterials, Brookhaven National Laboratory, was supported by the US Department of Energy, Office of Basic Energy Sciences, under Contract No. DE-AC02-98CH10886.

*jsimonson@bnl.gov

[1] I. I. Mazin, D. J. Singh, M. D. Johannes, and M. H. Du, Phys. Rev. Lett. **101**, 057003 (2008).

[2] K. Kuroki, S. Onari, R. Arita, H. Usui, Y. Tanaka, H. Kontani, and H. Aoki, Phys. Rev. Lett. **101**, 087004 (2008).

[3] J. Zhang, R. Sknepnek, R. M. Fernandes, and J. Schmalian, Phys. Rev. B **79**, 220502(R) (2009).

[4] D. N. Basov and A. V. Chubukov, Nat. Phys. **7**, 272 (2011).

[5] Y. Nakajima, T. Nakagawa, T. Tamegai, and H. Harima, Phys. Rev. Lett. **100**, 157001 (2008).

[6] R. Goto, S. Noguchi, and T. Ishida, Physica C **470**, S404 (2010).

[7] G. J. Smith, J. W. Simonson, T. Orvis, C. Marques, J. E. Grose, J. J. Kistner-Morris, L. Wu, Y. Zhu, V. O. Garlea, and M. C. Aronson (unpublished).

[8] J. D. Cashion, G. K. Shenoy, D. Niarchos, P. J. Viccaro, and C. M. Falco, Phys. Lett. A **79**, 454 (1980).

[9] J. D. Cashion, G. K. Shenoy, D. Niarchos, P. J. Viccaro, A. T. Aldred, and C. M. Falco, J. Appl. Phys. **52**, 2180 (1981).

[10] C. B. Vining and R. N. Shelton, Phys. Rev. B **28**, 2732 (1983).

[11] K. Momma and F. Izumi, J. Appl. Crystallogr. **41**, 653 (2008).

[12] J. H. Westbrook, R. K. DiCerbo, and A. J. Peat, General Electronic Research Laboratory Report No. 58-rc-2117, 1958.

[13]W. Jeitschko, A. G. Jordan, and P. A. Beck, Trans. Metall. Soc. AIME **245**, 335 (1969), and references therein.

[14]E. Horache, J. E. Fischer, and M. W. Ruckman, Phys. Rev. B **42**, 11079 (1990).

[15]H. Gretarsson, A. Lupascu, J. Kim, D. Casa, T. Gog, W. Wu, S. R. Julian, Z. J. Xu, J. S. Wen, G. D. Gu, R. H. Yuan, Z. G. Chen, N.-L. Wang, S. Khim, K. H. Kim, M. Ishikado, I. Jarrige, S. Shamoto, J.-H. Chu, I. R. Fisher, and Y.-J. Kim, Phys. Rev. B **84**, 100509(R) (2011).

[16]J. Rodriguez-Carvajal, Physica B **192**, 55 (1993).

[17]A. S. Wills, Physica B **276–278**, 680 (2000).

[18]P. Blaha, K. Schwarz, G. K. H. Madsen, D. Kvasnicka, and J. Luitz, WIEN2K, *An Augmented Plane Wave Plus Local Orbitals Program for Calculating Crystal Properties* (Karlheinz Schwarz, Techn. Universität Wien, Austria, 2001).

[19]J. P. Perdew, K. Burke, and M. Ernzerhof, Phys. Rev. Lett. **77**, 3865 (1996).

[20]J. Acker, K. Bohmhammel, G. J. K. van den Berg, J. C. van Miltenburg, and Ch. Kloc, J. Chem. Thermodyn. **31**, 1523 (1999).

[21]A. S. Wills, Phys. Rev. B **63**, 064430 (2001), and references therein.

[22]O. V. Kovalev, *Representations of the Crystallographic Space Groups*, 2nd ed. (Gordon and Breach, New York, 1993).

[23]D. M. Pajerowski, C. R. Rotundu, J. W. Lynn, and R. J. Birgeneau, Phys. Rev. B **87**, 134507 (2013).

[24]C. de la Cruz, Q. Huang, J. W. Lynn, J. Li, W. Ratcliff, J. L. Zarestky, H. A. Mook, G. F. Chen, J. L. Luo, N. L. Wang, and P. Dai, Nature (London) **453**, 899 (2008).

[25]P. Hansmann, R. Arita, A. Toschi, S. Sakai, G. Sangiovanni, and K. Held, Phys. Rev. Lett. **104**, 197002 (2010).

[26]Z. P. Yin, K. Haule, and G. Kotliar, Nat. Mater. **10**, 932 (2011).

[27]I. I. Mazin, M. D. Johannes, L. Boeri, K. Koepernik, and D. J. Singh, Phys. Rev. B **78**, 085104 (2008).

[28]K. Haule and G. Kotliar, New J. Phys. **11**, 025021 (2009).

[29]M. I. Aroyo, J. M. Perez-Mato, C. Capillas, E. Kroumova, S. Ivantchev, G. Madariaga, A. Kirov, and H. Wondratschek, Z. Krist. **221**, 15 (2006).

[30]K. Kadowaki and S. B. Woods, Solid State Commun. **58**, 507 (1986).

[31]K. Miyake, T. Matsuura, and C. M. Varma, Solid State Commun. **71**, 1149 (1989).

[32]A. C. Jacko, J. O. Fjaerestad, and B. J. Powell, Nat. Phys. **5**, 422 (2009).

[33]K. Hashimoto, A. Serafin, S. Tonegawa, R. Katsumata, R. Okazaki, T. Saito, H. Fukazawa, Y. Kohori, K. Kihou, C. H. Lee, A. Iyo, H. Eisaki, H. Ikeda, Y. Matsuda, A. Carrington, and T. Shibauchi, Phys. Rev. B **82**, 014526 (2010).

[34]A. S. Sefat, M. A. McGuire, B. C. Sales, R. Jin, J. Y. Howe, and D. Mandrus, Phys. Rev. B **77**, 174503 (2008).

[35]T. Okuda, W. Hirata, A. Takemori, S. Suzuki, S. Saijo, S. Miyasaka, and S. Tajima, J. Phys. Soc. Jpn. **80**, 044704 (2011).

[36]S. R. Julian, A. P. Mackenzie, G. G. Lonzarich, C. Bergemann, R. K. W. Haselwimmer, Y. Maeno, S. NishiZaki, A. W. Tyler, S. Ikeda, and T. Fujita, Physica B **259–261**, 928 (1999).